

Ring Type Structures in the Planck map of the CMB

Daniel An¹, Krzysztof A. Meissner² and Paweł Nurowski³

¹*Science Department SUNY Maritime College, 6 Pennyfield Av., New York 10465, USA*

²*Faculty of Physics, University of Warsaw, Pasteura 5, 02-093 Warsaw, Poland*

³*Center for Theoretical Physics of PAS, Al. Lotników 32/46, 02-688 Warsaw, Poland*

Abstract

We present the results of the quest for ring-type structures on the maps observed by the Planck satellite.

1 Introduction

The earliest optical image of the Universe we have is the cosmic microwave background – the earlier state of plasma precludes reaching further back. At almost the same time as the last recombination, perhaps not by coincidence, the pressure in the Universe decreased from one-third of its density to almost zero. The earlier structures, frozen till then because of pressure, started to evolve only after that. Therefore the density (temperature) profile obtained from the image gives us the wealth of information about much earlier epochs than the plasma-transparent Universe transition. In fact, because of the above-mentioned pressure, if the cosmic neutrino background is ever measured, we expect to observe similar maps to CMB even if neutrinos were released at time about 10 trillion times earlier than photons. Therefore a question of statistical properties of the CMB is of utmost importance for our understanding the very early Universe dynamics.

The usual inflationary paradigm with purely quantum mechanical fluctuations predicts absence of any large scale structures except the shape of the power spectrum. However, there are proposals, most notably Conformal Cyclic Cosmology (CCC) of Roger Penrose [1, 2], that predict presence of large scale structures, in this case ring-type. Discovery of any statistically significant structures imprinted in the CMB would contradict the usual inflationary paradigm independently of the question, whether they are a manifestation of CCC or not.

There remains, however, a fundamental problem of the definition of statistical significance of such structures in the case of our Universe: We have only one map. The map can be viewed and analyzed from different perspectives, in different frequency bands, and so on, but the situation is dramatically different from, say, particle physics where we can in principle get as many confidence level digits as we want at the expense of additional observational effort. The (dis)proof of the presence of such structures can therefore never be fully convincing and depends in an essential way on the initial assumptions.

The problem of finding structures in CMB maps was considered in a number of papers, in particular [3, 4, 5, 6, 7, 8], with conclusions sometimes disagreeing with each other. Our previous attempts, [9, 10], were devoted to the search of such structures on the WMAP and on the first release of the Planck data [11]. Neither the first one nor the second used the point source map to eliminate the known point sources on the sky that could have influenced the result. The results of [10] based on [11] seemed to have been a little inconsistent with [9] so with the release of the new data by the Planck collaboration [12] we have decided to carry out a new analysis and this paper reports the results.

In the present project we looked at ring-type structures in the real CMB temperature map in the frequency band 70 GHz as measured by the Planck collaboration as well as the foreground removed maps SMICA, SEVEM, NILC and Commander-Ruler. Rather than looking directly for ring structures, we present a case that certain cumulative distribution functions of the real maps are distinguished from that of the simulated maps generated by the HEALPix code [13].

The following is an outline of the procedure we have taken.

1. A grid of 49152 points with HEALPix $NSIDE = 64$ parametrization spreading over the entire celestial sphere has been created

2. For each of the points in the $NSIDE = 64$ grid, we put a disc of radius .42 radians and calculated how much the disc overlaps with the galactic mask and point source mask of the 70GHz map. The masks were obtained from Planck PR1 Ancillary Data. We chose only those centers which the overlap is less than 1%. This criteria gave us 14924 centers for the rings.
3. We were considering circles $C_{(i,\gamma)}$ with a spherical radius γ centered at the $N_d = 14924$ points (θ^i, ϕ^i) , $i = 1, 2, \dots, N_d$, from the grid on the sphere. Each circle $C_{(i,\gamma)}$ was surrounded by two rings - an inner ring $R_{(i,\gamma,\epsilon_-)}$, and an outer ring $R_{(i,\gamma,\epsilon_+)}$ - each of width ϵ . The inner (respectively, outer) ring consisted of $N_{(i,\gamma,\epsilon_-)}$ (respectively, $N_{(i,\gamma,\epsilon_+)}$) points, whose spherical angle from the point (θ^i, ϕ^i) was between $\gamma - \epsilon$ and γ (respectively, between γ and $\gamma + \epsilon$). The points in the rings were taken from the HEALPix grid with $NSIDE = 1024$, excluding all the points that belong to the galactic mask or the point source mask.
4. For each (θ^i, ϕ^i) , each $\gamma = 0.12, 0.14, 0.22, 0.24, 0.32, 0.34$ and a fixed width $\epsilon = 0.02, 0.04, 0.06$ and 0.08 , we calculated the difference between the average temperature in the inner ring and outer ring, i.e. the quantity

$$I_{(\gamma,\epsilon)}(\theta^i, \phi^i) = \sum_{\text{points in } R_{(i,\gamma,\epsilon_-)}} \frac{\delta T_m}{N_{(i,\gamma,\epsilon_-)}} - \sum_{\text{points in } R_{(i,\gamma,\epsilon_+)}} \frac{\delta T_m}{N_{(i,\gamma,\epsilon_+)}}$$

with δT_m being the temperatures at the points in the respective rings read from the 70GHz Planck map and foreground removed maps SMICA, SEVEM, NILC and Commander-Ruler. All maps were smoothed by cutting off frequency above $\ell > 1500$ to reduce noise, and resolution was downgraded to $NSIDE = 1024$ in order to reduce the computational load. Since 24 different combinations of radius and width were considered for 14924 centers, a total of 358176 integral values were computed per map.

5. For each γ 's we calculated the standard deviation σ_γ of the integral values and defined the normalization

$$\hat{I}(\gamma, \epsilon)(\theta^i, \phi^i) = I(\gamma, \epsilon)(\theta^i, \phi^i) / \sigma_\gamma. \quad (1)$$

This normalization was necessary in order to compare integral values between maps with different power spectra.

6. We chose a power spectrum and generated two sets of 1000 simulated maps using the HEALPix code with $NSIDE = 2048$, $l_{max} = 1500$ downgraded to $NSIDE = 1024$, so that the simulated maps underwent the same process as the real maps. The first 1000-maps set was generated with $fwhm=13$ arcmin which is the fwhm value of the Planck 70GHz map and the second 1000-maps set was generated with $fwhm=5$ arcmin which is the fwhm value of the foreground removed maps SMICA, SEVEM, NILC and Commander-Ruler. For each simulated maps, we computed the normalized integral values using the exactly same procedure used for the real map. The same masks were used for both the real map and the simulation maps.
7. From the normalized integral values of the simulated maps, we constructed cumulative distribution function $F_\gamma(\hat{I})$ for each radius γ .
8. For each simulated maps and the Planck maps, we computed A-values defined as ([14]):

$$A_{\gamma,R} = -\frac{a}{N_d} \sum_{i=1}^{N_d} \ln(1 - F_\gamma(\hat{I}_i)^a) \quad (2)$$

$$A_{\gamma,L} = -\frac{a}{N_d} \sum_{i=1}^{N_d} \ln(1 - (1 - F_\gamma(\hat{I}_i))^a) \quad (3)$$

where $a = 10000$ and I_i is the normalized integral values. The A-values enable us to compare the right and left tail of a CDF to another CDF [9]. Since we considered 24 different combinations of radius and width, each map gives us 48 A-values.

9. We took average of all A-values of a given map to come up with a single number per map, which enables us to compare between the Planck maps and the simulated maps.
10. we twisted the maps proportionally to the latitude with the twist parametrized by i , $i = 1, \dots, 8$ so that at the North (South) pole the twist was equal to $\theta = i\pi/8$ ($\theta = -i\pi/8$). This procedure emulates gradual change of circles into more and more elongated ellipses. The calculations for i from 0 (circles) to $i = 8$ were done for the most outstanding radius 0.14 with width 0.08.

We have used the A values introduced in [14] to compare the maps since it is very simple – it is just one number, sensitive to the right (left) end of the CDF (i.e. the extremal values of the integral give the biggest contributions to A) and it has established statistical properties (see [14]). The 70GHz map was compared with the simulated maps of $fwhm=13$ arcmin while the foreground-removed maps were compared with simulated maps of $fwhm=5$ arcmin.

This procedure was repeated for 5 different power spectra, two of which are from the 70GHz map and 3 of which are theoretical power spectra published by the Planck team. Since 2 sets of 1000 maps were generated for each power spectrum, total of 10000 simulated maps were compared to the Planck maps. The description of the power spectra is as follows:

1. Unbinned power spectrum: This is the power spectrum obtained from 70GHz map published by the Planck team.
2. Binned power spectrum: The power spectrum has been binned to generate a smooth change in the multipoles greater than $\ell = 50$. Cubic spline was used to get a smooth curve. For lower multipoles $\ell \leq 50$, this power spectrum is identical to the unbinned power spectrum
3. Theoretical power spectrum 1: Among the theoretical power spectrum published in Planck PR2 Ancillary data, this spectrum is base_plikHM.TTTEEE_lowTEB_lensing_post_BAO. The acronym is explained in [12]
4. Theoretical power spectrum 2: base_lensonly_BAO. See [12] for explanation.
5. Theoretical power spectrum 3: base_plikHM.TTTEEE_lowTEB_lensing_post_ BAO_H070p6_JLA. See [12] for explanation.

2 Results

The percentage of simulated maps that have higher A-value average than the given Planck map is given below as a table.

	Unbinned	Binned	Theoretical 1	Theoretical 2	Theoretical 3
70Ghz	3.5%	3.8%	3.6%	3.4%	6.0%
SMICA	5.7%	4.5%	4.7%	5.9%	4.7%
SEVEM	6.3%	5.2%	5.2%	6.5%	5.2%
NILC	6.2%	5.0%	5.0%	6.4%	5.0%
Commander	6.8%	5.6%	5.4%	7.0%	5.4%

Since each maps are being compared with a set of 1000 maps, 3.5% means there were 35 maps out of 1000 simulated maps that had higher A-value average than the 70GHz map.

Among the different radii, $\gamma = 0.14$ produced strong significance. The following table shows the significance for $\gamma = 0.14$ and $\epsilon = 0.08$.

	Unbinned	Binned	Theoretical 1	Theoretical 2	Theoretical 3
70Ghz	1.1%	0.9%	0.7%	0.8%	2.3%
SMICA	1.9%	1.7%	2.4%	2.4%	2.4%
SEVEM	2.0%	1.7%	2.5%	2.4%	2.5%
NILC	2.4%	1.7%	2.6%	2.6%	2.6%
Commander	2.4%	1.7%	2.6%	2.6%	2.6%

We plotted the rings which gave a high integral value, whose significance is judged by using the cumulative distribution functions obtained from the simulated maps generated from binned power spectrum.

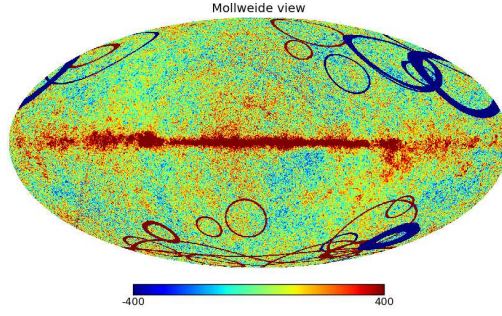


Figure 1: picture of 149 rings that have significance 0.0001, where $\text{radii}=[0.12,0.14,0.22,0.24,0.32,0.34]$ and $\text{width}=[0.02,0.04,0.06,0.08]$

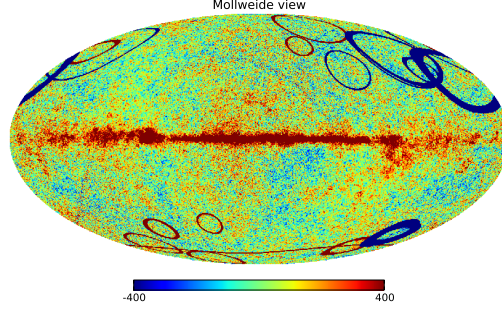


Figure 2: picture of 100 rings that have significance 0.00005, where $\text{radii}=[0.12,0.14,0.22,0.24,0.32,0.34]$ and $\text{width}=[0.02,0.04,0.06,0.08]$

Now, for any map, one may have rings of high integral values by pure chance. So it is important to compare the number of significant rings to expected number of significant rings. Since we are looking at 358176 rings of the map, we would expect about 71.6 ($= 358176 \times 0.0001 \times 2$) rings of significance 0.0001 and 35.8 rings of significance 0.00005. The fact that we find 103 rings at significance level of 0.00005, which is much more than the expected 35.8, suggests that these rings are not just statistical anomalies.

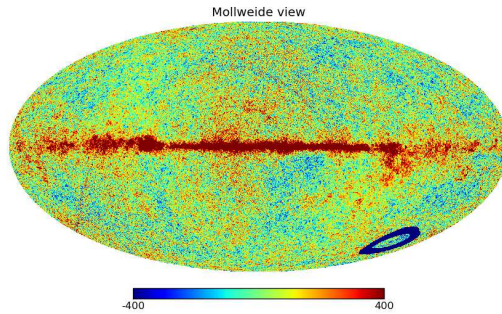


Figure 3: picture of the 15 rings with radius=0.14 and width =0.08 that have significance 0.0001

We also considered a different kind of normalization

$$\hat{I}(\gamma, \epsilon)(\theta^i, \phi^i) = (I(\gamma, \epsilon)(\theta^i, \phi^i) - \mu_\gamma) / \sigma_\gamma, \quad (4)$$

where μ_γ is the average value of the integrals. The results are not much different.

In the case of twisting (i.e. search for elongated ellipses) we can see below that they consistently and rapidly approach a purely statistical result with the growth of eccentricity:

Number of simulation maps whose $A_{\gamma=0.14}$ is higher than the real map for each twisting

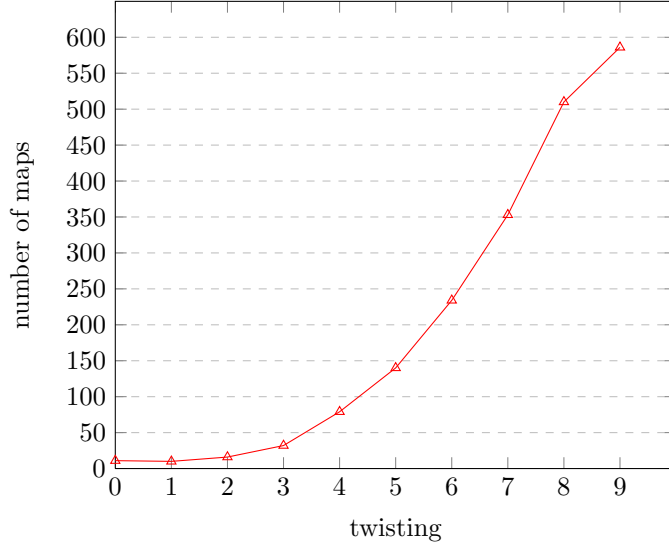


Table 1: Position, width and radius of some significant rings

Integral val	theta	phi	width	radius	sig%	1-sig%
-0.00008254	2.61237	3.73543	0.08	0.14	0.000030%	99.999970%
-0.00004316	0.92208	3.42385	0.02	0.32	0.000044%	99.999956%
-0.00004500	0.94797	3.39930	0.06	0.34	0.000332%	99.999668%
-0.00006492	0.84107	3.84109	0.04	0.14	0.000324%	99.999676%
0.00005838	2.74348	2.45754	0.02	0.14	99.999595%	0.000405%
0.00006783	2.54597	1.75861	0.04	0.12	99.999269%	0.000731%

3 Outlook

The results presented show that the probability that the ring-type structures are fluctuations is below 5% (1.9% to 3.8% for the 70 GHz map depending on the spectrum used). There are several directions in which one could extend the results in this paper. One of them could involve multiplying by the inverse correlation matrix to get rid of the correlations the other could involve more elaborate noise simulation. Both however are debatable whether the distortion to the data that they produce are indeed beneficial for the search of large scale structures – in our opinion the cleanest procedure is to use the least noisy map (i.e. 70 GHz) with the only necessary treatment involving removing the point sources. We hope that the description of the procedure used is sufficiently detailed to be useful for verifying the results presented in this paper. We have also checked the dependence of the results on the twist (proportional to the latitude) of both the artificial maps and the real map. The results show that the number of artificial maps that outperform the real map grows consistently and rapidly with the twisting angle showing that for this radius and width circles are distinguished.

Acknowledgments: We gratefully acknowledge helpful discussions with Paweł Bielewicz, Marek Demiański, Sigurd K. Næss, C. Denson Hill, George Efstathiou, E. Ted Newman, Roger Penrose and Błażej Ruszczycki. KAM was supported by the Polish NCN grant DEC-2013/11/B/ST2/04046, and PN by DEC-2013/09/B/ST1/01799.

References

- [1] R. Penrose, *Cycles of Time: An Extraordinary New View of the Universe*, Bodley Head, (2010)
- [2] V.G. Gurzadyan and R. Penrose, *On CCC-predicted concentric low-variance circles in CMB sky*, Eur. Phys. J. Plus **128**, 22 (2013)
- [3] P. Bielewicz, B.D. Wandelt and A.J. Banday, *A search for concentric rings with unusual variance in the 7-year WMAP temperature maps using a fast convolution approach*, Monthly Notices of the Royal Astronomical Society **429**, 1376 (2013)
- [4] A. DeAbreu, D. Contreras and D. Scott, *Searching for concentric low variance circles in the cosmic microwave background*, eprint arXiv:1508.05158, (2015)
- [5] A. Hajian, *Are there Echoes from the Pre-big-bang Universe? A Search for Low-variance Circles in the Cosmic Microwave Background Sky*, The Astrophysical Journal **740**, 52 (2011)
- [6] A. Moss, D. Scotta and J.P. Zibin, *No evidence for anomalously low variance circles on the sky*, Journal of Cosmology and Astroparticle Physics **4**, 33 (2011)
- [7] S.K. Næss, *Application of the Kolmogorov-Smirnov test to CMB data: Is the universe really weakly random?*, Astronomy & Astrophysics **538**, A17 (2012)
- [8] I.K. Wehus and H.K. Eriksen, *A Search for Concentric Circles in the 7 Year Wilkinson Microwave Anisotropy Probe Temperature Sky Maps*, The Astrophysical Journal Letters **733**, L29 (2011)
- [9] K.A. Meissner, P. Nurowski and B. Rusczycki, *Structures in the microwave background radiation*, Proc. R. Soc. **A469**:2155, 20130116 (2013)
- [10] D. An, K.A. Meissner and P. Nurowski, *Structures in the Planck map of the CMB*, eprint arXiv:1307.5737 (2013)
- [11] Planck Collaboration, *Planck 2013 results*, <http://planck.caltech.edu/publications2013Results.html>
- [12] 2015 Cosmological parameters and MC chains, http://wiki.cosmos.esa.int/planckpla2015/index.php/Cosmological_Parameters
- [13] K.M. Górski et al., *HEALPix: A Framework for High-Resolution Discretization and Fast Analysis of Data Distributed on the Sphere*, Astroph. J. **622** (2005) 759-771.
- [14] Meissner K. A., (2012) *A Tail Sensitive Test for Cumulative Distribution Functions*, arXiv:1206.4000 [math-st]

Table 2: 100 rings at 0.005% significant level: Out of 14924 centers* 6 radii* 4 widths=358176 rings considered, 100 rings achieved 0.00005 =0.005% significance, while 358176*0.0001=35.82 rings are expected to achieve such a level.

Integral val	theta	phi	width	radius	sig%	1-sig%
-0.00008254	2.61237	3.73543	0.08	0.14	0.000030%	99.999970%
-0.00004316	0.92208	3.42385	0.02	0.32	0.000044%	99.999956%
-0.00007735	2.62558	3.75028	0.06	0.14	0.000050%	99.999950%
-0.00007644	2.61237	3.73543	0.06	0.14	0.000077%	99.999923%
-0.00007814	2.61237	3.69712	0.08	0.14	0.000141%	99.999859%
-0.00007248	2.62558	3.71101	0.06	0.14	0.000164%	99.999836%
-0.00006610	2.61237	3.77374	0.04	0.14	0.000198%	99.999802%
-0.00007708	2.62558	3.71101	0.08	0.14	0.000237%	99.999763%
-0.00007706	2.59914	3.72129	0.08	0.14	0.000238%	99.999762%
-0.00007668	2.62558	3.75028	0.08	0.14	0.000272%	99.999728%
-0.00007613	2.59914	3.75869	0.08	0.14	0.000298%	99.999702%
-0.00006492	0.84107	3.84109	0.04	0.14	0.000324%	99.999676%
-0.00004500	0.94797	3.39930	0.06	0.34	0.000332%	99.999668%
-0.00006426	2.62558	3.75028	0.04	0.14	0.000378%	99.999622%
-0.00007034	2.61237	3.77374	0.06	0.14	0.000380%	99.999620%
-0.00007028	2.59914	3.75869	0.06	0.14	0.000396%	99.999604%
-0.00007537	2.61237	3.77374	0.08	0.14	0.000411%	99.999589%
-0.00006404	0.85496	3.82882	0.04	0.14	0.000412%	99.999588%
-0.00006830	2.61237	3.69712	0.06	0.14	0.000755%	99.999245%
-0.00004798	0.96074	3.38703	0.08	0.32	0.000773%	99.999227%
-0.00007337	2.58589	3.74434	0.08	0.14	0.000782%	99.999218%
-0.00006776	2.63876	3.72561	0.06	0.14	0.000861%	99.999139%
-0.00006178	2.61237	3.73543	0.04	0.14	0.000942%	99.999058%
-0.00004485	0.96074	3.41157	0.06	0.32	0.000960%	99.999040%
-0.00007946	2.61237	3.69712	0.08	0.12	0.000988%	99.999012%
-0.00005683	2.62558	3.75028	0.02	0.14	0.001004%	99.998996%
-0.00004506	0.94797	3.39930	0.08	0.34	0.001103%	99.998897%
-0.00007891	2.58589	3.74434	0.08	0.12	0.001133%	99.998867%
-0.00004222	0.94797	3.42385	0.06	0.34	0.001159%	99.998841%
-0.00004475	0.93509	3.38703	0.08	0.34	0.001202%	99.998798%
-0.00007855	2.62558	3.71101	0.08	0.12	0.001241%	99.998759%
-0.00007847	2.59914	3.72129	0.08	0.12	0.001259%	99.998741%
-0.00006636	2.58589	3.74434	0.06	0.14	0.001303%	99.998697%
-0.00007144	2.62558	3.67174	0.08	0.14	0.001310%	99.998690%
-0.00006569	2.59914	3.72129	0.06	0.14	0.001575%	99.998425%
-0.00006041	2.59914	3.75869	0.04	0.14	0.001600%	99.998400%
-0.00004359	0.94797	3.39930	0.06	0.32	0.001626%	99.998374%
-0.00007065	2.57261	3.76634	0.08	0.14	0.001653%	99.998347%
-0.00007727	2.62558	3.67174	0.08	0.12	0.001684%	99.998316%
-0.00003828	0.96074	3.43612	0.04	0.34	0.001695%	99.998305%
-0.00004129	0.93509	3.41157	0.06	0.34	0.001729%	99.998271%
-0.00006536	0.84107	3.84109	0.06	0.14	0.001750%	99.998250%
-0.00005509	2.61237	3.77374	0.02	0.14	0.001751%	99.998249%
-0.00007713	2.59914	3.75869	0.08	0.12	0.001751%	99.998249%
-0.00004109	0.93509	3.38703	0.06	0.34	0.001927%	99.998073%
-0.00004306	0.96074	3.38703	0.06	0.32	0.002060%	99.997940%
-0.00004364	0.96074	3.41157	0.08	0.34	0.002063%	99.997937%
-0.00006988	2.63876	3.72561	0.08	0.14	0.002068%	99.997932%
-0.00004583	0.96074	3.41157	0.08	0.32	0.002080%	99.997920%
-0.00007617	2.61237	3.73543	0.08	0.12	0.002107%	99.997893%
-0.00004256	0.84107	4.94555	0.02	0.22	0.002463%	99.997537%
-0.00003749	0.94797	3.42385	0.04	0.34	0.002526%	99.997474%
-0.00006416	2.57261	3.76634	0.06	0.14	0.002530%	99.997470%
-0.00004319	0.93509	3.41157	0.08	0.34	0.002602%	99.997398%
-0.00004046	0.96074	3.38703	0.06	0.34	0.002605%	99.997395%
-0.00005823	2.63876	3.72561	0.04	0.14	0.002879%	99.997121%
-0.00004279	0.94797	3.42385	0.08	0.34	0.003033%	99.996967%
-0.00004489	0.94797	3.39930	0.08	0.32	0.003035%	99.996965%
-0.00007452	2.63876	3.68533	0.08	0.12	0.003079%	99.996921%
-0.00004197	0.68975	3.98627	0.06	0.32	0.003135%	99.996865%
-0.00006934	2.59914	3.72129	0.06	0.12	0.003200%	99.996800%
-0.00006335	2.63876	3.68533	0.06	0.14	0.003294%	99.996706%
-0.00004183	0.93509	3.41157	0.06	0.32	0.003302%	99.996698%
-0.00004467	0.97339	3.39930	0.08	0.32	0.003356%	99.996644%
-0.00007412	2.61237	3.65881	0.08	0.12	0.003368%	99.996632%
-0.00003503	0.63578	2.83705	0.02	0.32	0.003482%	99.996518%
-0.00004164	0.68975	3.95663	0.06	0.32	0.003522%	99.996478%
-0.00004164	0.67621	3.97230	0.06	0.32	0.003523%	99.996477%
-0.00004157	0.94797	3.37476	0.06	0.32	0.003608%	99.996392%
-0.00006859	2.58589	3.74434	0.06	0.12	0.003752%	99.996248%
-0.00004425	0.94797	3.37476	0.08	0.32	0.003908%	99.996092%
-0.00004420	0.68975	3.95663	0.08	0.32	0.003980%	99.996020%
-0.00006708	2.61237	3.65881	0.08	0.14	0.004144%	99.995856%
-0.00006698	2.58589	3.78087	0.08	0.14	0.004273%	99.995727%
-0.00003931	0.94797	3.37476	0.06	0.34	0.004331%	99.995669%
-0.00003767	0.96074	3.41157	0.04	0.32	0.004381%	99.995619%
-0.00003761	0.93509	3.41157	0.04	0.32	0.004465%	99.995535%
-0.00004380	0.97339	3.37476	0.08	0.32	0.004645%	99.995355%
-0.00006195	2.58589	3.78087	0.06	0.14	0.004786%	99.995214%
-0.00006189	2.62558	3.67174	0.06	0.14	0.004857%	99.995143%
-0.00004182	0.70333	3.99971	0.08	0.34	0.004882%	99.995118%
-0.00007216	2.57261	3.76634	0.08	0.12	0.004894%	99.995106%
-0.00004080	0.70333	3.97062	0.06	0.32	0.004909%	99.995091%
-0.00006632	2.63876	3.68533	0.08	0.14	0.004949%	99.995051%
0.00006656	2.79541	4.10152	0.06	0.12	99.995376%	0.004624%
0.00003422	3.07779	3.61283	0.02	0.32	99.995599%	0.004401%
0.00005656	2.47889	0.84700	0.02	0.12	99.996153%	0.003847%
0.00005674	2.54597	1.79276	0.02	0.12	99.996316%	0.003684%
0.00005698	0.55571	5.53432	0.02	0.12	99.996580%	0.003420%
0.00005306	0.62237	2.92888	0.02	0.14	99.997034%	0.002966%
0.00006843	2.78245	4.06724	0.06	0.12	99.997238%	0.002762%
0.00006326	2.78245	4.06724	0.04	0.12	99.997277%	0.002723%
0.00006399	2.76947	4.08949	0.04	0.12	99.997720%	0.002280%
0.00006410	2.78245	4.12334	0.04	0.12	99.997773%	0.002227%
0.00005436	0.63578	2.93322	0.02	0.14	99.998106%	0.001894%
0.00005877	2.97555	1.75204	0.02	0.12	99.998124%	0.001876%
0.00006014	0.63578	2.93322	0.04	0.14	99.998323%	0.001677%
0.00004406	0.29449	4.88313	0.02	0.22	99.998680%	0.001320%
0.00006783	2.54597	1.75861	0.04	0.12	99.999269%	0.000731%
0.00005838	2.74348	2.45754	0.02	0.14	99.999595%	0.000405%